Progressive parkinsonism in mice with respiratory-chain-deficient dopamine neurons

Mats I. Ekstrand[†], Mügen Terzioglu[†], Dagmar Galter[‡], Shunwei Zhu[§], Christoph Hofstetter[‡], Eva Lindqvist[‡], Sebastian Thams[‡], Anita Bergstrand[‡], Fredrik Sterky Hansson[†], Aleksandra Trifunovic[†], Barry Hoffer[¶], Staffan Cullheim[‡], Abdul H. Mohammed[§], Lars Olson[‡], and Nils-Göran Larsson[†‖]

[†]Department of Laboratory Medicine and [§]Neurotec, Karolinska Institutet, Karolinska University Hospital, S-14186 Stockholm, Sweden; [‡]Department of Neuroscience, Karolinska Institutet, S-17177 Stockholm, Sweden; and [¶]National Institute on Drug Abuse, National Institutes of Health, 5500 Nathan Shock Drive, Baltimore, MD 21224

Mitochondrial dysfunction is implicated in the pathophysiology of Parkinson's disease (PD), a common age-associated neurodegenerative disease characterized by intraneuronal inclusions (Lewy bodies) and progressive degeneration of the nigrostriatal dopamine (DA) system. It has recently been demonstrated that midbrain DA neurons of PD patients and elderly humans contain high levels of somatic mtDNA mutations, which may impair respiratory chain function. However, clinical studies have not established whether the respiratory chain deficiency is a primary abnormality leading to inclusion formation and DA neuron death, or whether generalized metabolic abnormalities within the degenerating DA neurons cause secondary damage to mitochondria. We have used a reverse genetic approach to investigate this question and created conditional knockout mice (termed MitoPark mice), with disruption of the gene for mitochondrial transcription factor A (Tfam) in DA neurons. The knockout mice have reduced mtDNA expression and respiratory chain deficiency in midbrain DA neurons, which, in turn, leads to a parkinsonism phenotype with adult onset of slowly progressive impairment of motor function accompanied by formation of intraneuronal inclusions and dopamine nerve cell death. Confocal and electron microscopy show that the inclusions contain both mitochondrial protein and membrane components. These experiments demonstrate that respiratory chain dysfunction in DA neurons may be of pathophysiological importance in PD.

inclusion | mitochondria | mtDNA | neurodegeneration | Parkinson

The mtDNA encodes 13 key subunits of the respiratory chain and mtDNA expression is therefore critical for mitochondrial biogenesis (1). Mutations of mtDNA cause a variety of neurodegenerative phenotypes in humans and mitochondrial dysfunction has also been implicated in common forms of age-associated neurodegenerative diseases (2). Indirect evidence suggests a role for mitochondrial dysfunction in sporadic PD (2). In addition, studies of families with rare inherited forms of PD have identified genes involved in regulating mitochondrial function (3–5). Additional support comes from experimental studies with toxins that inhibit complex I of the mitochondrial respiratory chain and cause death of midbrain DA neurons (6). However, the interpretation of results from experiments with neurotoxins is complicated by the fact that they may have pleiotropic pharmacological effects in dopamine (DA) neurons, effects on non-DA cell types, or both (6). The hypothesis that mitochondrial dysfunction may be of etiological importance in PD has recently gained renewed attention because it has been shown that PD patients have an increased fraction of respiratory chain deficient DA neurons (7). Normal aging is associated with accumulation of somatic mtDNA mutations and appearance of scattered cytochrome *c* oxidase (COX)-deficient cells in a variety of organs (8, 9). Analysis of individual COX-deficient cells has demonstrated that they often contain high levels of mtDNA with somatically acquired deletions or point mutations (8, 9). Studies of mtDNA mutator mice expressing an error prone version of the catalytic subunit of mitochondrial DNA polymerase have provided additional experimental evidence that high levels of somatic mtDNA mutations directly can cause a variety of aging phenotypes in mammals (10).

Analysis of mtDNA mutation levels in DA neurons with normal COX activity has demonstrated very high levels of mtDNA with deletions in both PD patients and aged controls and there was a linear increase of the mutation load with increasing age (7). The somatic mtDNA mutation levels in midbrain DA neurons were much higher than these levels in other types of neurons (7). The same study reported ≈3% COX deficient DA neurons in the midbrain of PD patients, whereas the levels were much lower in age-matched controls (7). There is a progressive loss of midbrain DA neurons during normal aging (11), and the observed accumulation of somatic mtDNA mutations may cause a respiratory chain deficiency that contributes to this cell loss (7).

Studies of human tissues can only generate correlative data, and it is therefore important to experimentally test the hypothesis that mitochondrial dysfunction may be an etiological factor in Parkinson's disease (PD). One way of investigating this issue is to create mice with a tissue-specific respiratory chain deficiency in midbrain DA neurons. Efficient disruption of respiratory chain function can be accomplished in selected cell types of the mouse by using a *loxP*-flanked allele for mitochondrial transcription factor A (*Tfam*[loxP]) in conjunction with tissue-specific *cre*-recombinase expression (12–18). The TFAM protein is necessary for mtDNA maintenance in mammals (12, 19) and regulates mtDNA copy number by directly binding and coating mtDNA (19). In addition, TFAM is absolutely required for transcription initiation at mtDNA promoters (20). We report here that mice with tissue-specific knockout of *Tfam* develop severe respiratory chain deficiency in DA neurons with adult onset of slowly progressive typical parkinsonian features. Our findings thus provide experimental support for the hypothesis that acquired respiratory chain dysfunction may be of pathophysiological importance in PD.

Results

Creation of *DAT-cre* Mice. To direct *cre*-recombinase expression to DA neurons, we first introduced the *cre*-gene together with the
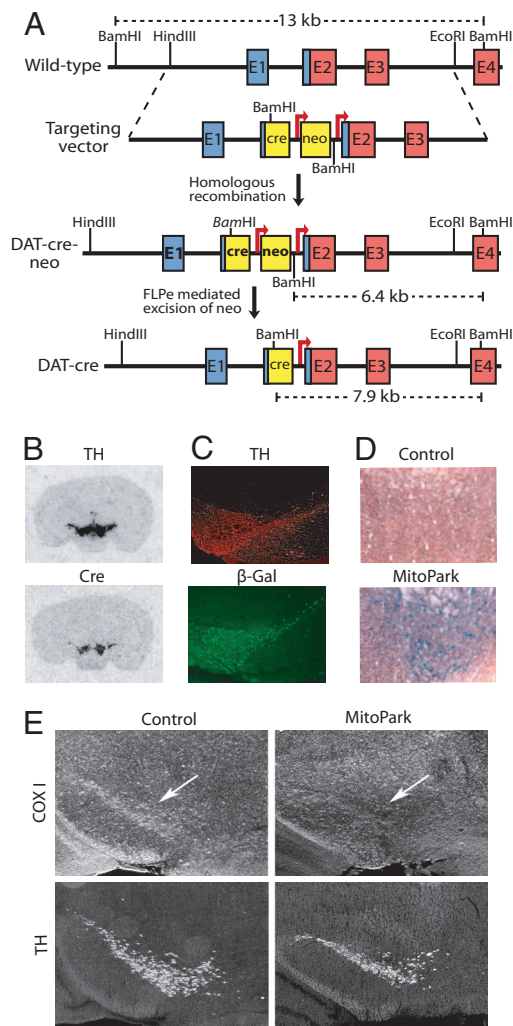
MEDICAL SCIENCES

Fig. 1. Creation of MitoPark mice. (*A*) Creation of DAT-cre mice. A cassette containing an *NLS-cre* (cre) gene followed by an *FRT*-flanked (arrows) *neomycin* (neo) gene was inserted upstream of the translation start codon in exon 2. The *neo* gene was removed by breeding to FLPe deleter mice. Noncoding exon sequence is blue, and coding sequence is red. (*B*) *In situ* hybridization of midbrain dopamine neurons. Probes detecting TH and *cre* mRNA showed overlapping hybridization signals in SN and VTA of a heterozygous *DAT-cre* mouse. (*C*) Immunohistochemistry of a ROSA26-R reporter mouse containing the *DAT-cre* knock-in allele. The *cre* protein expression activates β-galactosidase protein expression in a pattern that overlaps with TH protein expression in SN and VTA. (*D*) Cytochrome *c* oxidase (COX) activity in a 20-week-old control mouse is normal in VTA, whereas there is dramatic decrease in COX activity (blue staining represents COX deficient neurons) in a MitoPark mouse of the same age. (*E*) *In situ* hybridization shows decreased expression of the cytochrome *c* oxidase subunit I (COX I) mRNA in DA neurons of the midbrain (arrow) of a 6-week-old MitoPark mouse (*Upper Right*) in comparison with a control (*Upper Left*). *In situ* hybridization was performed to detect TH mRNA expression in DA neurons of SN and VTA in adjacent sections (*Lower*).

neomycin resistance gene into the dopamine transporter (DAT) locus (21) and obtained heterozygous *DAT-cre-neo* mice (Fig. 1*A*). Next, we excised the neomycin gene by *in vivo* Flp-Frt-mediated recombination (22) and obtained heterozygous *DAT-cre* mice (Fig. 1*A*). We used *in situ* hybridizations (Fig. 1*B*) and mating to reporter mice (23), which activate the expression of β-galactosidase in *cre*-expressing cells (Fig. 1*C*), to establish that *DAT-cre* mice express *cre* mRNA and enzymatically active *cre*-recombinase protein in DA neurons of the midbrain.

Mice with Reduced mtDNA Expression in Midbrain DA Neurons. We crossed *DAT-cre* mice and mice with a *loxP*-flanked *Tfam* allele (*Tfam*^{loxP}) to produce MitoPark mice (genotype +/*DAT-cre*, *Tfam*^{loxP}/*Tfam*^{loxP}) with homozygous disruption of *Tfam* in midbrain DA neurons. *In situ* hybridizations detected much reduced expression of the mtDNA-encoded COX subunit I mRNA in DA neurons of substantia nigra (SN) and the ventral tegmental area (VTA) in MitoPark mice at the age of 6 weeks (Fig. 1*E*). We also found a marked reduction of COX enzyme activity by histochemical analyses of midbrain DA neurons of 20-week-old MitoPark mice (Fig. 1*D*). These findings show that there is a severe reduction of mtDNA expression, which, in turn, causes a severe respiratory chain deficiency in midbrain DA neurons of MitoPark mice.

Adult Onset of DA-Responsive Progressive Parkinsonism. There was no increased embryonic or neonatal lethality in MitoPark mice. Decreased locomotion and reduced exploratory behavior first became apparent at age ≈14–15 weeks. We observed progression of symptoms with tremor, increased twitching and apparent limb rigidity at age ≈20 weeks and MitoPark mice had to be killed at ≈45 weeks of age because of poor general condition. We performed behavioral tests to obtain quantitative measurements of the clinically obvious motor impairment in MitoPark mice and found progressive decline of both locomotion (Fig. 2 *A–C*) and rearing (Fig. 2*D*) in MitoPark mice from the age of 14 weeks. A single dose of L-DOPA markedly improved motor performance (Fig. 2 *E–G*) and, interestingly, an identical L-DOPA dose elicited a more pronounced and longer lasting locomotion response in younger in comparison with older MitoPark mice (Fig. 2 *E* and *F*). The locomotor response abruptly terminated in the older MitoPark mice, resembling the "wearing off" effect seen in advanced PD (Fig. 2*E*).

Progressive Loss of Midbrain DA Neurons and Striatal DA Nerve Terminals. Loss of DA innervation was first observed in dorsolateral striatum at age 12 weeks and this loss progressed to involve most of the dorsal and ventral striatum as the MitoPark mice became older (Fig. 3 *A–D*). Quantification of numbers of tyrosine hydroxylase (TH)-expressing midbrain neurons revealed a slow progressive cell loss, which was more marked and had an earlier onset in SN, which predominantly innervates dorsal striatum, in comparison with VTA, which predominantly innervates ventral striatum and cortical areas (Fig. 3 *E–I*). This differential degeneration is also characteristic of PD in man. We performed neurochemical studies, which confirmed that the DA nerve cell loss resulted in a corresponding loss of DA in different parts of the nigrostriatal system of 20-week-old MitoPark mice (Fig. 3 *J* and *K*). We also found markedly increased ratios of the DA metabolites homovanillic acid (HVA) and 3,4-dihydroxyphenylacetic acid (DOPAC), to DA in striatum of 20-week-old MitoPark mice (Fig. 3*L*), consistent with increased DA turnover typically seen in DA deficiency and in human PD.

Intraneuronal Inclusions Associated with Mitochondria. In 6-week-old MitoPark mice, there was no observable DA cell loss (Fig. 3*F*) despite the presence of severely reduced mtDNA expression (Fig. 1*E*) in midbrain DA neurons. However, the DA neurons did not appear normal at this clinically presymptomatic stage, as a majority of them contained small cytoplasmic aggregates (Fig. 4 *A–D*). A polyclonal antibody raised against a peptide of human α-synuclein (h116–131), was strongly immunoreactive with the intraneuronal inclusions. However, five additional antibodies (see *Methods*) directed against α-synuclein were not immunoreactive with the inclusions although they gave rise to expected α-synuclein-like immunoreactivity in nonaffected neurons. These results raised questions about the specificity of the h116–131 α-synuclein antibody to detect mouse α-synuclein and we
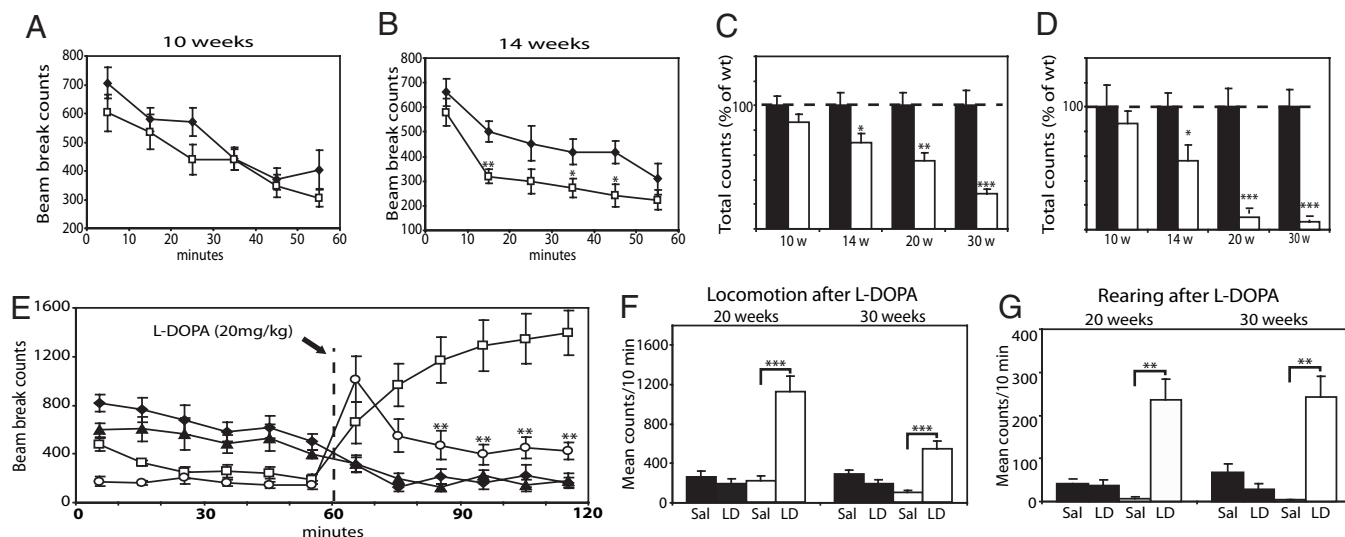
Fig. 2. Analysis of spontaneous activity and motor function in MitoPark mice. (*A–D*) Locomotion and rearing of MitoPark (white dots/bars; *n* = 8) and control mice (black dots/bars; *n* = 7) were measured for 60 min in open-field activity cages. Locomotion in 10-week-old MitoPark mice was not significantly different from age-matched controls (*A*), whereas 14-week-old MitoPark mice displayed decreased locomotion (*B*). Total locomotion (*C*) and total rearing (*D*) during 60 min decreased with increasing age in MitoPark mice (*n* = 12), but not in age-matched controls (*n* = 12). Error bars indicate ± SEM. Statistically significant differences to age-matched controls are indicated as: *, $P < 0.05$; **, $P < 0.01$; ***, $P < 0.001$. (*E–G*) Cohorts of 20- and 30-week-old MitoPark (white dots/bars; *n* = 12) and control mice (black dots/bars; *n* = 15) were treated with L-DOPA (20 mg/kg) or saline. (*E*) Locomotion in controls at age 20 weeks (black squares), controls at age 30 weeks (black triangles), MitoPark mice at age 20 weeks (white circles), and MitoPark mice at age 30 weeks (white circles). MitoPark mice of both ages responded to L-DOPA treatment with increased locomotion (*E* and *F*) and rearing (*G*). L-DOPA treatment of younger MitoPark mice resulted in a greater locomotion response than treatment of older MitoPark mice (*E*). L-DOPA has no effect in control mice (*E* and *F*). The increase of rearing after L-DOPA treatment of MitoPark mice was similar in both age groups (*G*). Mean ± SEM is indicated by bars. The bars show mean locomotion (*F*) and mean rearing (*G*) in control and MitoPark mice treated with saline (Sal) or L-DOPA (LD). Statistically significant differences are indicated: *, $P < 0.05$; **, $P < 0.01$; ***, $P < 0.001$.

therefore bred MitoPark mice to α-synuclein knockout mice (24). The absence of a functional α-synuclein gene had no obvious impact on the phenotype in MitoPark mice (data not shown). Unexpectedly, the inclusions also remained, and were immunoreactive with the h116–131 antibody in the MitoPark mice lacking a functional α-synuclein gene (data not shown). We thus conclude that the inclusions do not contain α-synuclein and that the h116–131 antibody reacted with an unknown component of the inclusions. Thus α-synuclein was neither needed for the PD phenotype nor the development of DA neuron inclusions in our mice. Due to its excellent signal-to-noise characteristics in

detecting the inclusions, we used the h116–131 antibody for further studies of the abundance and location of such inclusions in the degenerating DA neurons. The inclusions were present in most midbrain DA neurons (Fig. 4*C*) and their mean size increased as neurodegeneration progressed (Fig. 4*D*). Inclusions were not found in non-DA neurons. Ultrathin sections from the midbrain of MitoPark and control mice at age 11 weeks were examined by electron microscopy. In MitoPark mice only, we observed large, clearly delineated and partially electron-dense bodies often located in dendritic structures close to neuronal somata (Fig. 5). Some of these bodies had an amorphous content
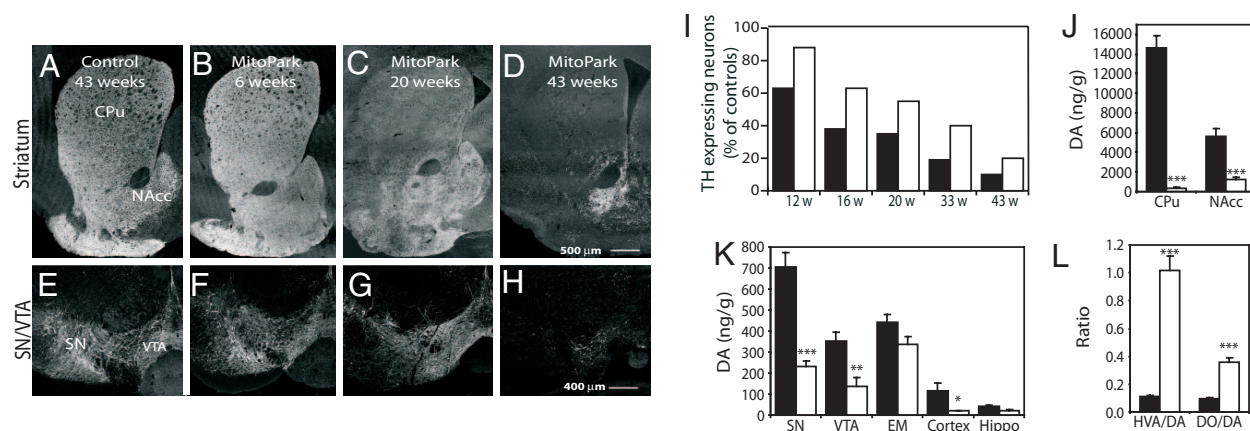
Fig. 3. TH immunohistochemistry and DA levels in the midbrain of MitoPark mice. (*A–D*) TH immunoreactivity in striatum of control (*A*) and MitoPark mice (*B–D*). (*E–H*) TH immunoreactivity in SN and VTA of control (*E*) and MitoPark (*F* and *G*) mice. (*I*) Quantitative assessment of cell loss in SN (black bars) and VTA (white bars) of MitoPark mice at different ages. (*J* and *K*) Measurement of DA and DA metabolite levels. DA levels in striatum (*J*) and other brain regions (*K*) of 20-week-old control (black bars) and MitoPark (white bars) mice. EM, eminentia mediana (=A12 area), hippo: the hippocampal formation. (*L*) Ratios of the DA metabolites HVA and DOPAC (DO) to DA in striatum of 20-week-old control (black bars) and MitoPark (white bars) mice. Error bars indicate ± SEM. Statistically significant differences to age-matched controls are indicated as: *, $P < 0.05$; **, $P < 0.01$; ***, $P < 0.001$.
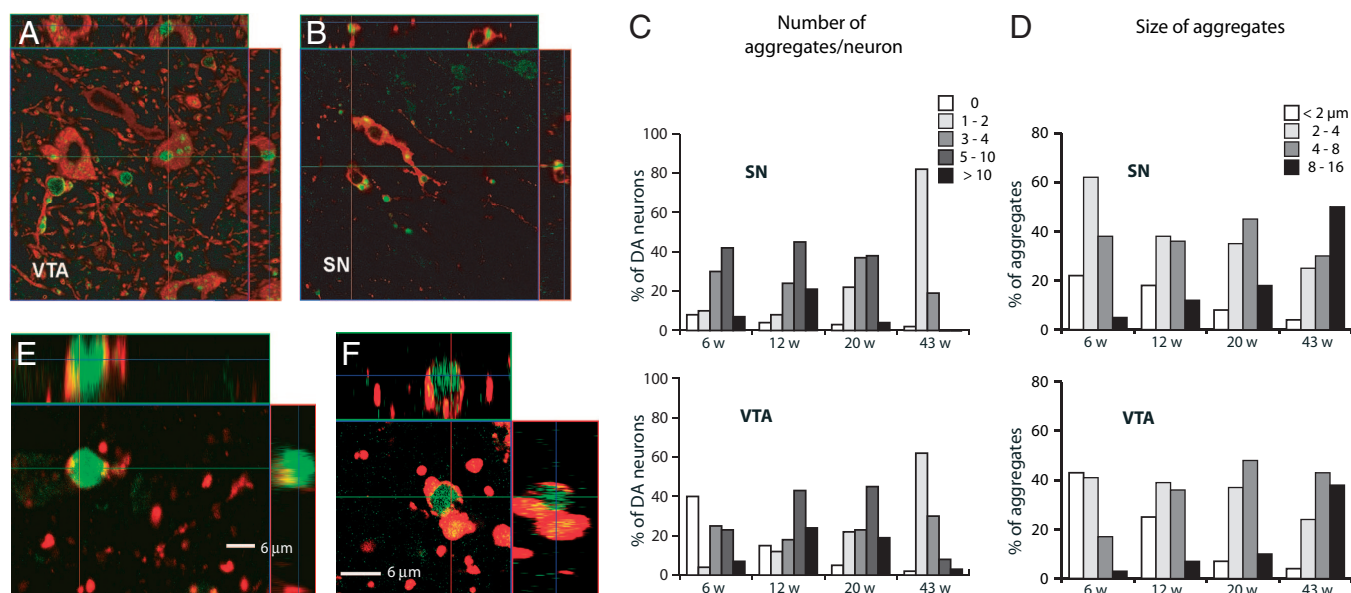
Fig. 4. Analysis of intracellular inclusions. (*A* and *B*) Confocal microscopy images of immunoreactive inclusions (green) in TH immunoreactive DA neurons (red) of VTA and SN. (*C*) Quantification of number of aggregates per DA neuron in SN and VTA of MitoPark mice at different ages. (*D*) Size of aggregates in DA neurons in SN and VTA of MitoPark mice at different ages. (*E* and *F*) High magnification confocal images of aggregates after double immunofluorescence labeling to detect inclusions (green) and mitochondria (red).

and a diffuse lining, whereas others displayed tubular formations and were surrounded by distinct double layer membranes (Fig. 5 *B* and *C*). We even observed what appeared to be transitional states, wherein a portion of the body had started to become dense with a diffuse border and the other portion still maintained its membrane and tubular system (Fig. 5*C*). The double membrane structures incorporated into the inclusions were ultrastructurally typical of mitochondrial membranes and we therefore performed immunolabeling of tissue sections followed by confocal microscopy. We found many examples where a mitochondrial marker protein, the nucleus-encoded α-subunit of mitochondrial ATP synthase, partially overlapped with, was juxtaposed to, or even surrounded the inclusions (Fig. 4 *E* and *F*). These data strongly suggest that dysfunctional mitochondria have a direct role in the formation of the intracytoplasmic inclusions.

Discussion

We demonstrate that respiratory chain deficiency in DA neurons in mice leads to characteristic manifestations of parkinsonism, including slowly progressive neuronal degeneration, typical behavioral disturbances, and the formation of intraneuronal inclusions. We present evidence that dysfunctional mitochondria directly participate in inclusion formation. However, we did not find evidence of α-synuclein in these inclusions, although α-synuclein is commonly found in Lewy bodies in human PD. Indeed, the inclusions readily formed even in MitoPark mice lacking functional α-synuclein genes. Available data show that Lewy bodies can have a variety of morphological shapes (25), and it has been suggested that their morphology evolves with time (25). Studies by others have suggested that there may be a possible interaction between α-synuclein and mitochondria. *In vitro* studies have shown that α-synuclein can interact directly with lipids found in membranes (26, 27) and with proteins of the mitochondrial respiratory chain (28, 29). The morphology of Lewy bodies has mainly been studied in brain tissue obtained from end-stage PD patients, and it is therefore not well established how these aggregates appear at early disease stages.

The mechanism whereby respiratory chain deficiency leads to inclusion formation in MitoPark mice needs to be elucidated. Previous studies have suggested that formation of reactive oxygen species and oxidative stress is of importance in PD. However, there is no absolute link between respiratory chain dysfunction and oxidative stress. We have studied a variety of mouse models with decreased mtDNA expression (10, 12–18) and such mice have increased cell death with little or no increase of oxidative stress (18, 30). It should therefore be emphasized that a possible mitochondrial etiology for PD does not automatically mean that reactive oxygen species and oxidative stress are of major importance.

Function of the respiratory chain depends on the coordinated expression of both mtDNA and nuclear genes, and a balanced expression of both genomes is necessary for proper assembly of the multisubunit respiratory chain enzyme complexes. The mitochondrial network has an elaborate system for protein degradation involving membrane bound AAA-proteases and LON protease in the matrix (31). Reduced mtDNA expression leads to an excess of nucleus-encoded respiratory chain subunits that must be degraded by the mitochondrial proteolytic system. Gene expression studies in a mouse model with progressive cardiomyopathy, induced by tissue-specific *Tfam* knockout causing mtDNA depletion, has demonstrated a strong induction of LON-protease expression (14). We speculate that reduced mtDNA expression may lead to an aggregation of nucleus-encoded proteins in mitochondria of DA neurons and that this event could initiate an aggregation process also involving non-mitochondrial proteins.

In summary, we present genetic evidence, using transgenic techniques, that a primary deficiency of respiratory chain function in midbrain DA neurons leads to the progressive development of key PD features in the mouse: (*i*) adult onset of neurodegeneration, (*ii*) slowly progressive clinical course, (*iii*) formation of intraneuronal inclusions (*iv*) earlier onset of cell death and more extensive cell death in SN than in VTA, and (*v*) responsiveness to L-DOPA therapy with a differential response depending on disease stage. Previous mouse models have not reproduced all of these characteristic features of PD, and the

Fig. 5. Electron micrographs illustrating the morphology of intraneuronal inclusions. (*A*) An inclusion (arrow) in a nerve cell with nucleolus-containing nucleus (arrowhead). (*B*) A cluster of five abnormal mitochondria and inclusions containing mitochondrial membranes. (*C*) High magnification of a single inclusion of mixed morphology, which is located in a dendrite (delineated by dashed line). The amorphous portion of the inclusion shows diffuse lining and dissolved membrane whereas the more intact portion of the body show tubular structures and a visible double layer membrane. A bouton making synaptic contact with the dendrite is indicated by an asterisk.

MitoPark mice may therefore provide a platform to study key pathophysiological events in PD. In addition, our results provide experimental support for the hypothesis that reduced mtDNA expression may be an etiological event in PD.

Materials and Methods

Construction of *DAT-cre* Mice. DNA clones containing the 5′-end of the dopamine transporter gene (DAT) were obtained from a 129/SvJ λ Fix II phage library (Stratagene, La Jolla, CA). A ≈3.7-kb sequence extending from upstream of exon 1 and downstream from intron 5 was released with NotI and subcloned into pBlueScript II SK, generating pME1. An *NLS-cre/FRT-neo-FRT* cassette was constructed by subcloning the needed elements in several steps. First, the multiple cloning site cassette of pBlueScript II SK was released with SalI–KpnI and replaced with a synthetic oligo containing an FRT recombination site and necessary restriction enzyme sites (SacI/PacI/SalI/EcoRI/KpnI/ FRT-sequence/XhoI/EcoRI/SacII/AscI/KpnI*), thus generating

pME2. The KpnI site of pME2 was inactivated during the cloning procedure. A DNA fragment encoding *NLS-cre* was released from pML78 (Mark B. Lewandoski, National Cancer Institute, Frederick, MD) using SalI–KpnI and ligated into pME2, generating pME3. Next, a synthetic oligo containing an *FRT*-sequence was introduced after the polyadenylation site in pMC1neo–poly(A) (provided by Thomas Perlmann, Karolinska Institutet), using BamHI and SacII. This *neo-FRT* construct was then released with XhoI–SacII and ligated into pME3, generating pME4. For final assembly of the targeting construct a new plasmid was generated by replacing the MCS of pBlueScript II SK with an oligo containing restriction sites for the insertion of 5′ and 3′ homology arms as well as for the *NLS-cre/FRT-neo-FRT* cassette (SacI/NotI/BamHI/SmaI/PacI/BamHI/AscI/EcoRV/ BamHI/EcoRI/KpnI), generating pME5. The 5′ and 3′ homology arms were released from pME1 with NotI–FspI and FspI–EcoRI, respectively, and inserted into pME5 using NotI–SmaI and EcoRV–EcoRI. The cassette from pME4 was released and inserted between the homology arms using PacI–AscI. The endogenous DAT translational start site is located in exon 2 and the plasmid we constructed introduces a cassette in intron 1. Finally, we introduced a short synthetic oligonucleotide to recreate the sequence of the intron 1/exon 2 border at the PacI site, which is 5′ to the introduced *cre* gene, generating pME6. The targeting vector was linearized with NotI and electroporated into R1 embryonic stem (ES) cells. To remove the *FRT*-flanked *neo* gene downstream of the *cre* gene, mice heterozygous for the targeted DAT-locus (*+/DAT-cre-neo*) were mated to FLPe deleter mice.

***In Situ* Hybridization.** Oligonucleotide probes to detect transcripts encoding tyrosine hydroxylase (5′-GGT GTG CAG CTC ATC CTG GAC CCC CTC CAA GGA GCG CT-3′), cre recombinase (5′-GCC CGG ACC GAC GAT GAA GCA TGT TTA GCT GGC CCA AAT GTT GCT GGA-3′ or 5′-CAC CAG AGA CGG AAA TCC ATC GCT CGA CCA GTT TAG TTA CCC CCA GGC-3′) and Cox I (TGG GTC CCC TCC TCC AGC GGG ATC AAA GAA AGT TGT GTT TAG GTT GCG G) were labeled with ^{33}P and used for radioactive *in situ* hybridizations (16).

Histology and Immunohistochemistry. Mice were perfused with Ca^{2+}-free Tyrode's solution, followed by 4% paraformaldehyde with 0.4% picric acid in 0.16 M phosphate buffer. The brains were dissected out, postfixed, and equilibrated to 10% sucrose containing 0.1% sodium azide. Primary antibodies used for indirect immunohistochemistry (16) included polyclonal antibodies against TH (1:400; Pel-Freez, Rogers, AR), β-galactosidase (1:500; Chemicon, Temecula, CA) and the nucleus-encoded α-subunit of mitochondrial ATP synthase (1:250; Molecular Probes, Eugene, OR). Several different antibodies were used to detect α-synuclein: (*i*) the polyclonal goat anti-human peptide 116–131 antibody (1:100; Biogenesis, Poole, U.K.), (*ii*) Syn-1, a monoclonal mouse anti rat 15–123 antibody recognizing human and mouse α-synuclein (1:500; BD Biosciences, San Jose, CA), (*iii*) Syn- 202, a mouse monoclonal antibody directed to human α-synuclein peptide 130–140, recognizing human and mouse α- and β-synuclein (1:400; Abcam, Cambridge, U.K.), (*iv*) Syn 4D6, a monoclonal mouse anti-recombinant human α-synuclein (1:300; Abcam), (*v*) a polyclonal rabbit anti human peptide 111–131 antibody (1:2,000; Chemicon), and (*vi*) a polyclonal sheep anti-human peptide 108–120 antibody (1:1,000; Chemicon). A total of seven pairs of Mitopark mice and control littermates at different ages were used for *in situ* hybridization studies and enzyme histochemical stainings and 20 pairs of mice at different ages for immunohistochemistry. TH-immunoreactive DA nerve cell body profiles were counted on coded slides at representative levels of SN and

VTA, respectively, using two to five sections per animal and a total of 18 mice (nine littermate pairs, each consisting of one MitoPark and one control). Average numbers of SN and VTA cells/section and animal were compared. We counted the number of aggregates in 100 representative DA cells per time point, area and animal in a total of nine animals. We identified cells by TH and h116–131 antibody double labeling. To determine size distribution of the aggregates, we measured the largest diameter of a minimum of 100 individual aggregates/time point, area and animal in a total of nine animals using appropriate software. To determine colocalization patterns, confocal microscopy (LSM 510 Meta; Zeiss, Jena, Germany) was used.

Electron Microscopy. Mice were perfused with 2% glutaraldehyde in 440 mM Millonig's buffer (pH 7.4), and brains were removed. A 1-mm-thick section containing SN was dissected out from each brain. The surrounding tissue was removed and the section was cut in the midline, so that each piece contained the left or right SN. Each SN was cut into three pieces of 1–2 mm^3 and postfixed in 2% glutaraldehyde solution. The specimens were then further trimmed, osmicated, dehydrated, and embedded in Durcupan (Fluka, Buchs, Switzerland). Ultrathin sections from SN were collected on formvar-coated copper grids, contrasted with uranyl acetate and lead citrate, and examined by using an electron microscope (CM12; Philips, Eindhoven, The Netherlands).

Behavioral Analyses of Animals. Open-field activity was examined in automated activity cages. Animals were tested during the light phase of the light–dark cycle, between 0900 and 1300 h. Locomotor activity was registered when animals interrupted a lower row of photocells and rearing was registered when upper row photocells were interrupted. Animals were individually placed gently in the open-field arena and remained there for 60 min. Locomotion and rearing counts were registered every 10 min. For the L-DOPA treatment, spontaneous locomotion and rearing were measured in activity cages for 60 min as above. Animals were then given i.p. injections of either L-DOPA combined with the peripheral dopa decarboxylase inhibitor benserazide (Madopark 20 mg/kg in PBS; Roche, Basel, Switerland) or PBS and were then immediately put back into the activity cages for another 60 min of recording. The scoring of counts was given as mean ± SEM. Statistical significance was tested by using two-way ANOVA analysis.

Catecholamine Measurements. High-pressure liquid chromatography (HPLC) with electrochemical detection was used to measure catecholamines and metabolites in striatum and mesencephalon (32).

1. Gaspari M, Larsson NG, Gustafsson CM (2004) *Biochim Biophys Acta* 1659:148–152.
2. Dauer W, Przedborski S (2003) *Neuron* 39:889–909.
3. Shen J, Cookson MR (2004) *Neuron* 43:301–304.
4. Park J, Lee SB, Lee S, Kim Y, Song S, Kim S, Bae E, Kim J, Shong M, Kim JM, Chung J (2006) *Nature* 441:1157–1161.
5. Clark IE, Dodson MW, Jiang C, Cao JH, Huh JR, Seol JH, Yoo SJ, Hay BA, Guo M (2006) *Nature* 441:1162–1166.
6. Smeyne RJ, Jackson-Lewis V (2005) *Brain Res Mol Brain Res* 134:57–66.
7. Bender A, Krishnan KJ, Morris CM, Taylor GA, Reeve AK, Perry RH, Jaros E, Hersheson JS, Betts J, Klopstock T, et al. (2006) *Nat Genet* 38:515–517.
8. Cottrell DA, Blakely EL, Johnson MA, Ince PG, Borthwick GM, Turnbull DM (2001) *Neurobiol Aging* 22:265–272.
9. Taylor RW, Barron MJ, Borthwick GM, Gospel A, Chinnery PF, Samuels DC, Taylor GA, Plusa SM, Needham SJ, Greaves LC, et al. (2003) *J Clin Invest* 112:1351–1360.
10. Trifunovic A, Wredenberg A, Falkenberg M, Spelbrink JN, Rovio AT, Bruder CE, Bohlooly Y-M, Gidlöf S, Oldfors A, Wibom R, et al. (2004) *Nature* 429:417–423.
11. Volkow ND, Gur RC, Wang GJ, Fowler JS, Moberg PJ, Ding YS, Hitzemann R, Smith G, Logan J (1998) *Am J Psychiatry* 155:344–349.
12. Larsson NG, Wang J, Wilhelmsson H, Oldfors A, Rustin P, Lewandoski M, Barsh GS, Clayton DA (1998) *Nat Genet* 18:231–236.
13. Wang J, Wilhelmsson H, Graff C, Li H, Oldfors A, Rustin P, Brüning JC, Kahn CR, Clayton DA, Barsh GS, Thoren P, Larsson NG (1999) *Nat Genet* 21:133–137.
14. Hansson A, Hance N, Dufour E, Rantanen A, Hultenby K, Clayton DA, Wibom R, Larsson NG (2004) *Proc Natl Acad Sci USA* 101:3136–3141.
15. Silva JP, Kohler M, Graff C, Oldfors A, Magnuson MA, Berggren PO, Larsson NG (2000) *Nat Genet* 26:336–340.
16. Sorensen L, Ekstrand M, Silva JP, Lindqvist E, Xu B, Rustin P, Olson L, Larsson NG (2001) *J Neurosci* 21:8082–8090.
17. Wredenberg A, Wibom R, Wilhelmsson H, Graff C, Wiener HH, Burden SJ, Oldfors A, Westerblad H, Larsson NG (2002) *Proc Natl Acad Sci USA* 99:15066–15071.
18. Wang J, Silva J, Gustafsson CM, Rustin P, Larsson NG (2001) *Proc Natl Acad Sci USA* 98:4038–4043.
19. Ekstrand MI, Falkenberg M, Rantanen A, Park CB, Gaspari M, Hultenby K, Rustin P, Gustafsson CM, Larsson NG (2004) *Hum Mol Genet* 13:935–944.
20. Falkenberg M, Gaspari M, Rantanen A, Trifunovic A, Larsson NG, Gustafsson CM (2002) *Nat Genet* 31:289–294.
21. Donovan DM, Vandenbergh DJ, Perry MP, Bird GS, Ingersoll R, Nanthakumar E, Uhl GR (1995) *Brain Res Mol Brain Res* 30:327–335.
22. Dymecki SM (1996) *Proc Natl Acad Sci USA* 93:6191–6196.
23. Soriano P (1999) *Nat Genet* 21:70–71.
24. Cabin DE, Shimazu K, Murphy D, Cole NB, Gottschalk W, McIlwain KL, Orrison B, Chen A, Ellis CE, Paylor R, Lu B, Nussbaum RL (2002) *J Neurosci* 22:8797–8807.
25. Shults CW (2006) *Proc Natl Acad Sci USA* 103:1661–1668.
26. Cole NB, Murphy DD, Grider T, Rueter S, Brasaemle D, Nussbaum RL (2002) *J Biol Chem* 277:6344–6352.
27. Ellis CE, Murphy EJ, Mitchell DC, Golovko MY, Scaglia F, Barcelo-Coblijn GC, Nussbaum RL (2005) *Mol Cell Biol* 25:10190–10201.
28. Hashimoto M, Takeda A, Hsu LJ, Takenouchi T, Masliah E (1999) *J Biol Chem* 274:28849–28852.
29. Elkon H, Don J, Melamed E, Ziv I, Shirvan A, Offen D (2002) *J Mol Neurosci* 18:229–238.
30. Trifunovic A, Hansson A, Wredenberg A, Rovio AT, Dufour E, Khvorostov I, Spelbrink JN, Wibom R, Jacobs HT, Larsson NG (2005) *Proc Natl Acad Sci USA* 102:17993–17998.
31. Rugarli EI, Langer T (2006) *Trends Mol Med* 12:262–269.
32. Andersson H, Luthman J, Lindqvist E, Olson L (1995) *Neurotoxicology* 16:201–210.